Negative Impedance Boosting

By L. A. MEACHAM

(Manuscript received February 6, 1968)

Linearized and feedback-stabilized negative impedance circuits having only R, C, and solid state components, powered in series at intervals along a cable pair, offer new possibilities in bilateral transmission. After discussing the basic negative impedance boosting units and the transmission characteristics they impart to a line (computed, with experimental confirmation), this paper describes a field test of two 32-mile telephone lines, largely 22-gauge, each having an insertion loss of only 3 dB at 1,000 Hz. It also shows means for broadening bandwidth and almost eliminating delay distortion over negative impedance boosted lines. Treatment of this sort adapts them to unusual uses. Examples include converting rectangular to raised-cosine pulses in transmission, without pulse-forming circuitry, and the bilateral two-wire transmission of carrier or pulse signals in both directions simultaneously, without frequency separation.

I. INTRODUCTION

The insertion of lumped negative impedances at intervals along each conductor of a cable pair has long been of interest as a means of improving bilateral transmission. In the familiar expressions for propagation constant

$$\gamma = \alpha + j\beta = \sqrt{(R + j\omega L)(G + j\omega C)} \tag{1}$$

and characteristic impedance

$$Z_0 = R_0 + jX_0 = \sqrt{(R + j\omega L)/(G + j\omega C)}, \tag{2}$$

if one lets both G and R go to zero on presumption that the shunt conductance of well-insulated cable is negligible and that the copper resistance can effectively be canceled by active devices, he encounters four challenging approximations:

$$\alpha \approx 0, \qquad \beta \approx \omega\sqrt{LC}, \qquad R_0 \approx \sqrt{L/C} \quad \text{and} \quad X_0 \approx 0. \tag{3}$$

To the extent of their accuracy these describe lossless transmission, free of phase distortion, between matching terminations that are resistive and independent of frequency. Such properties would indeed be of value in either analog or digital transmission.*

In the early 1940s effort toward canceling R was devoted to high speed point-contact thermistors as the requisite "current-controlled" or "open-circuit-stable" negative impedance elements,[2] but lack of stability and uniformity were severe obstacles. Similar handicaps were later encountered with other devices such as avalanche transistors.[3] At least partly for such reasons, development eventually tended to abandon the scheme of distributing bilateral active elements along a pair over which they could also be powered, and instead moved toward combinations of shunt and series type negative impedances (transformer coupled, locally powered, and designed to match the cable in characteristic impedance) that could be installed at convenient points such as in central offices, and there contribute modest amounts of bilateral gain. A well-known outcome was the E-type repeater,[4] of which both vacuum-tube and transistor versions have found extensive use in the exchange plant of the Bell System.

Recently, however, a new look has been taken at negative impedance boosting† (NIB). This paper outlines in chronological order various findings of a small research project that has been in progress for several years at Bell Laboratories.

II. BASIC NIB CIRCUIT

An NIB unit devised early in this study and used as a basic tool appears schematically in Fig. 1. Figure 2 shows its d-c V-I characteristic and equivalent circuit. For convenience the latter represents the total impedance Z_A of a pair of units, one in series with each conductor, at a boosting point.

Accordingly, for small currents (below the first bend of the characteristic) $-R_n = +2R_3$ and $R_p = 4R_2$. At that bend the silicon transistors begin to conduct, while at the second bend they saturate.

* As early as 1887 Oliver Heaviside defined a "distortion constant" $(R/L - G/C) = 2\sigma$ and an "attenuation constant" $(R/L + G/C) = 2\delta$, and showed that distortion could be "annihilated" by increasing G to make $G/C = R/L$[1]. He undoubtedly would have stressed the benefits of making both σ and δ approach zero, had he known of any way to reduce R except the use of more copper.

† "Boosting" is proposed as a better term than "loading," on the grounds that the mass/inductance analogy suggested by the latter is irrelevant.

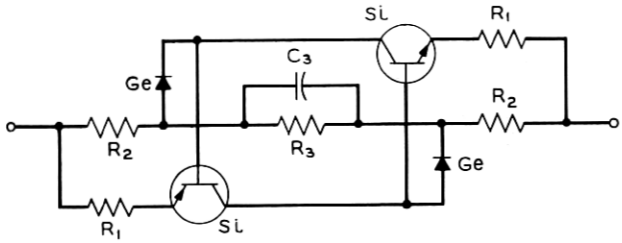

Fig. 1 — Circuit schematic of basic negative impedance booster unit.

In the active region between bends simple circuit analysis shows that

$$R_p = \frac{4R_1R_2}{R_1 + R_2}, \tag{4}$$

$$-R_n = -2R_3\left[\frac{R_2(2\alpha - 1) - R_1}{R_1 + R_2}\right], \tag{5}$$

and

$$-C_n = \frac{R_3C_3}{-R_n}. \tag{6}$$

Here α, the usual ratio of collector to emitter current, is assumed constant and the same for both transistors. Expression (5) tacitly takes into account the nonlinearity of the emitter junctions in Fig. 1; this follows from the fact that the voltage across each emitter junction is compensated, except for an approximately constant voltage difference of about 0.5 volt, by the drop across a germanium junction diode carrying a proportional and almost equal current. The 0.5-volt difference, inherent between silicon and germanium, effectively affords a bias essential to the circuit. The drop across R_2 equals this bias at the first bend, and to a close approximation exceeds the drop across R_1 by the same value of 0.5 volt throughout the active region. The important result of this compensation is a high degree of linearity between the bends, which correspondingly are sharpened almost into cusps.

III. BASIC NIB LINE

Some basic features of an NIB line are illustrated in the telephone customer's loop of Fig. 3. The boosters have a spacing that is (preferably) regular and not much greater than one quarter wavelength at the top of the transmission band. For telephone speech, a suitable

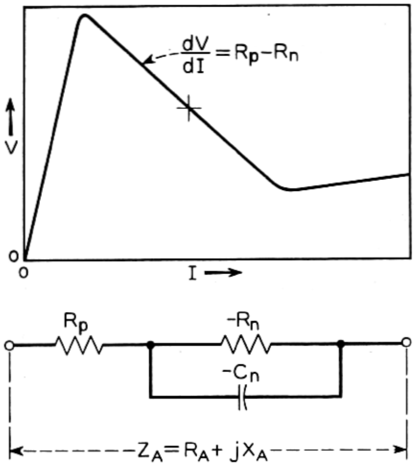

Fig. 2 — DC characteristic and equivalent circuit of basic NIB unit.

spacing would be 12,000 feet. In general, boosting gives the line a characteristic impedance substantially lower than that of ordinary nonloaded or inductively loaded telephone lines. Hence the line circuit at the central office includes an impedance-matching transformer, as well as means for regulating the d-c loop current roughly at the center of the active region of the V-I characteristic. The telephone set can be conventionally powered by this current, and should have a resistive impedance, preferably matching that of the line.

Stability criteria are well known[5] for such arrangements. In practical terms, for regularly spaced NIB units with the equivalent circuit of Fig. 2, the system is found stable (experimentally and by computer) when the net d-c variational resistance ($\Delta V/\Delta I$) of the loop, including its terminations, is positive, provided that the time constant $T_n = R_n C_n$ is greater than a certain critical value. In this study (except where noted) we have consistently made

$$\Sigma R = lR + R_p - R_n = 0,$$

where R is the copper resistance per unit length of cable and l is the NIB spacing. The negative capacitor $-C_n$ bypasses $-R_n$, and with rising frequency gradually reduces the negative real component of terminal impedance of the NIB unit. One way of visualizing the need for such reduction is to notice that the positive copper resistance adjacent to each of the four terminals of the two NIB units at a boosting point is also effectively reduced, being bypassed by the mutual line capacitance. Hence with rising frequency, a point of instability is almost certain to be reached unless the negative resistance diminishes at least as fast as the copper resistance as seen from the NIB terminals.

T_n is therefore an important parameter of the NIB circuit. Increasing it raises the margin of stability, but at the penalty of reducing transmission bandwidth. The midspacing image impedance of the line is also affected by T_n. It is found that when the line conductance per section (lG) is negligible, and when the line resistance per section (lR) is exactly compensated by $R_p - R_n$, the midspacing image impedance Z_H remains essentially constant and resistive as the frequency falls toward zero. As shown in the Appendix, the value it thus approaches is given precisely by

$$Z' = \lim_{\omega \to 0} Z_H = \sqrt{\frac{R_n T_n}{lC} + \frac{L}{C} - \frac{R^2 l^2}{12}} \tag{7}$$

where R, L and C are the usual primary cable constants (per unit length). R_p enters (7) implicitly, being the difference between R_n and lR.

A related effect of T_n is upon the phase velocity $V_H = \omega/\beta_H$, which also approaches an asymptotic value:

$$V' = \lim_{\omega \to 0} V_H = \frac{1}{CZ'}. \tag{8}$$

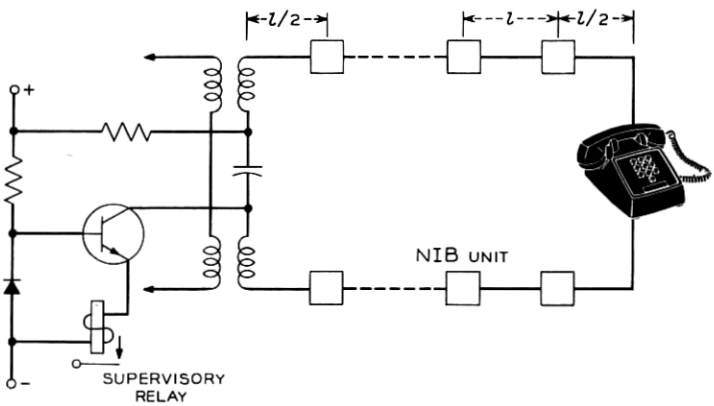

Fig. 3 — Negative impedance boosted subscriber line and central office terminating circuit.

Expressions (7) and (8) are useful, for the values they give hold approximately over a major part of the low-loss frequency band. As an example, take the case of 12,000-foot (2.2727-mile) NIB spacing, along 22-gauge BSA cable that has the primary constants (at low frequency) $R = 173$ ohms per mile, $L = 0.874 \times 10^{-3}$ henry per mile, and $C = 0.825 \times 10^{-6}$ farad per mile. For the NIB parameters (per section) $R_p = 97.3$ ohms, $R_n = 490.5$ ohms, and $T_n = 16 \times 10^{-6}$ second, expressions (7) and (8) tell us

$$Z' = 198 \text{ ohms}$$

and

$$V' = 61{,}200 \text{ miles per second.}$$

For this velocity, the spacing becomes a quarter wavelength at the frequency

$$f_{\lambda/4} = V'/4l = 6{,}730 \text{ Hz.}$$

IV. COMPUTED CHARACTERISTICS

Computer programs have been worked out to give propagation constant and midspacing image impedance as functions of frequency, for any set of cable primary "constants" (which of course actually vary with frequency) and NIB equivalent circuit parameters. Some typical results, plotted in Figs. 4, 5, 6, apply to the set of parameters used in the foregoing example. For comparison, characteristics are included for nonloaded (NL) and loaded (H88) cable, also of 22 gauge. (H88 loading uses 88 mH inductors at 6,000-foot intervals.)

Among varied uses of these programs has been the finding, by successive approximations, of the minimum or "just stable" time constant (jstc) for various gauges and NIB spacings. Figure 7 shows attenuation constant versus frequency for the jstc condition and also for a time constant 10 per cent greater. To illustrate another use, the effect upon attenuation of moderate over- or undercompensation is pictured in Fig. 8. Here the loss per mile between image impedances is shown for errors in compensation of ±20 ohms, or approximately ±5 per cent of the copper resistance. Over most of the useful band, these errors introduce almost flat gain or loss of about 0.2 dB per mile. Their effects upon phase velocity and image impedance (not plotted) are small except at frequencies below 500 Hz.*

* In that region the variation of image impedance is such that if Fig. 8 were a plot of insertion loss between 198-ohm resistive terminations, it would show the gain or loss of 0.2 dB per mile extending almost unchanged all the way down to zero frequency.

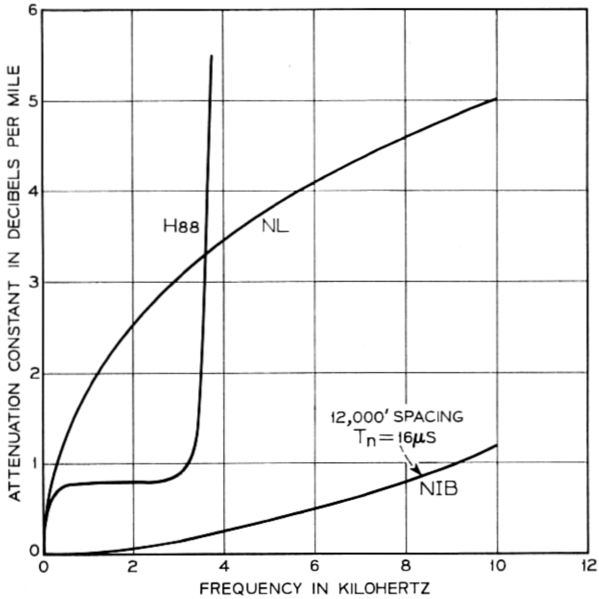

Fig. 4 — Attenuation constant of 22-gauge BSA cable; nonloaded, H-88 loaded, and negative impedance boosted.

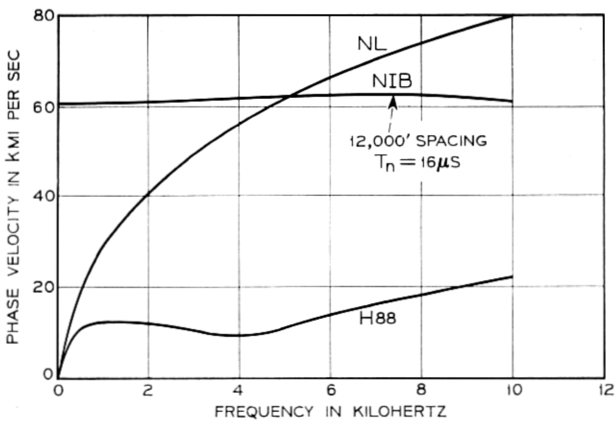

Fig. 5 — Phase velocity of 22-gauge BSA cable; nonloaded, H-88 loaded and negative impedance boosted.

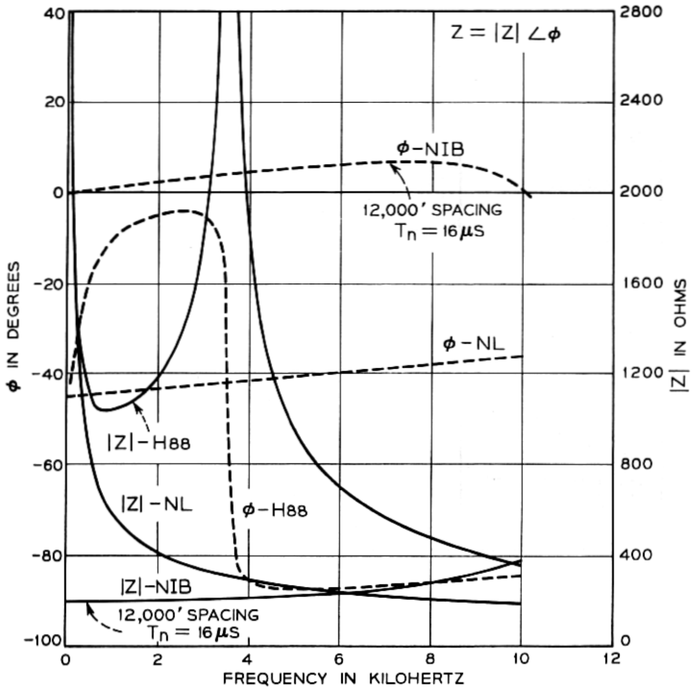

Fig. 6 — Characteristic impedance or midspacing image impedance of 22-gauge BSA cable; nonloaded, H-88 loaded, and negative impedance boosted.

In general, our laboratory tests using either dependably representative artificial lines, or pairs in actual cable on spools, confirmed the computed results very accurately. Conversation over lines several 12,000-foot NIB sections in length was found highly satisfactory—remarkably free of hum, echo, and distortion. But the need was seen for experience with NIB transmission under actual field conditions.

V. "ROUND ROBIN" FIELD TEST

With the cooperation of the New Jersey Bell Telephone Company two NIB lines were set up using pairs in existing interoffice cables over the route shown in Fig. 9. For convenience of measurement, both ends of each line were brought to the same room at the Murray Hill, New Jersey, branch of Bell Laboratories. Experimental applique circuits were provided for coupling to the Murray Hill PBX, permitting each pair to serve as a regular telephone extension when not in use for other tests.

The cable, 32.4 miles long, was all of 22 gauge except for 0.5 per cent of 24 and 4.2 per cent of 26 gauge. Seventy-seven per cent of its length was underground, the rest aerial. All boosting points, one for each of 16 sections ranging from 9,750 to 13,380 feet long, were in manholes. There the NIB units were plugged into jacks within containers that could be conveniently opened and resealed, taking advantage of equipment already installed (for housing regenerative repeaters of the T1 type PCM transmission system).

The NIB circuits were adapted to field conditions in the following ways:

(*i*) By giving R_3 an appropriate positive temperature coefficient, the net coefficient of each NIB unit was matched approximately to that of copper. It was recognized that this compensation would be reasonably accurate for underground cable, but little better than seasonal for aerial.

(*ii*) Taps were provided along R_3 so that any one of four values of

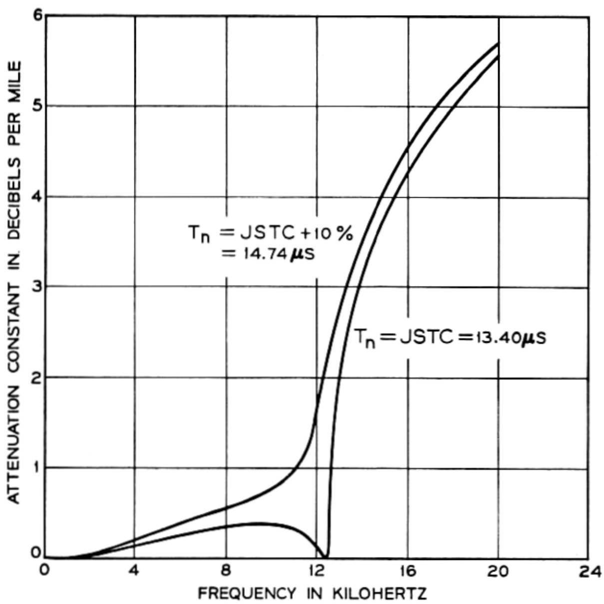

Fig. 7 — Attenuation constant of line with NIB time constant at or near "just stable" value; 22-gauge BSA cable, NIB spacing 12,000 feet.

$-R_n$ could be selected by strapping, as a best fit for the section resistance. No corresponding adjustment of C_3 proved necessary, as the image impedance fortunately turned out to be kept almost constant by the related changes in T_n, $-R_n$ and l.

(*iii*) To increase stability margins in view of the nonuniform NIB spacing, T_n was raised to 20μs for the mean length of 22-gauge section. This gave an image impedance Z' of 225 ohms.

(*iv*) For the two end sections of each line, which happened to include all the 26-gauge cable, T_n was adjusted by changing the capacitor C_3 (Fig. 1) to make the image impedance roughly equal to that of other sections (225 ohms).

Except for these adjustments, the NIB units had the equivalent circuit parameters listed in the discussion of expressions (7) and (8). They were normally powered by 16 mA of loop current, with their linear negative slopes extending from 6 to 26 mA. This range was

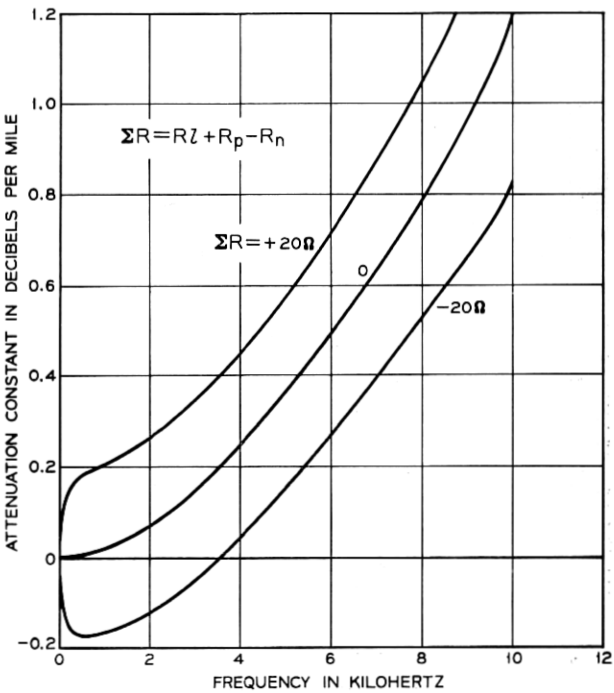

Fig. 8 — Effect of over- or undercompensation of copper resistance; 22-gauge BSA cable, spacing 12,000 feet, 16μs time constant.

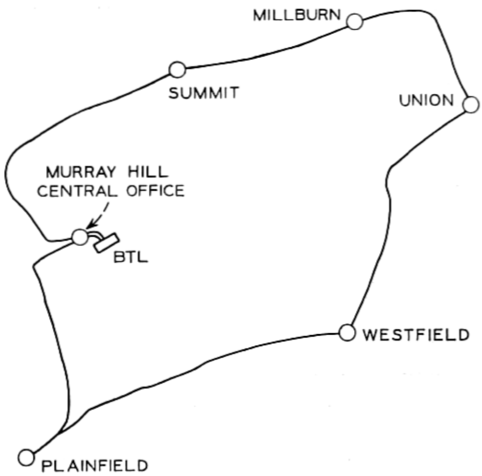

Fig. 9 — Cable route in field test of negative impedance boosting. The line was 32 miles long, mostly buried 22 gauge cable, and it had 16 NIB sections.

twice as great as required for telephone speech; the excess was an allowance for possible hum current. The total IR drop in copper and NIB units of either loop was about 186 volts; hence, with an additional 4-volt drop across a 225-ohm resistive station set, the potentials on tip and ring conductors at the "office end" were approximately ±95 volts from ground.

Touch-Tone® calling was used on one line, rotary dialing on the other. The severe distortion occurring when the rotary dialing pulses were produced by complete interruption of loop current was remedied by having the dial merely insert enough resistance to drop the current from 16 to 6 mA (the regulator going out of range). With the NIB thus left operative, dial pulse distortion became negligible.

Tone ringing[6] was used on both lines, the signal being a 1,000 Hz wave interrupted at 10 Hz. This was applied with a level of about 1 mW at the applique line circuit, under control of the ordinary ringing signal from the PBX.

Supervision was conventional. The current regulator was so designed that when the path was broken by the switchhook the open-circuit voltage on the loop did not greatly exceed the ±95 volt figure. A relay in the applique, responding to the switchhook (and dial pulses) transferred the information to the PBX pair.

The performance of the NIB lines was gratifying. People conversing

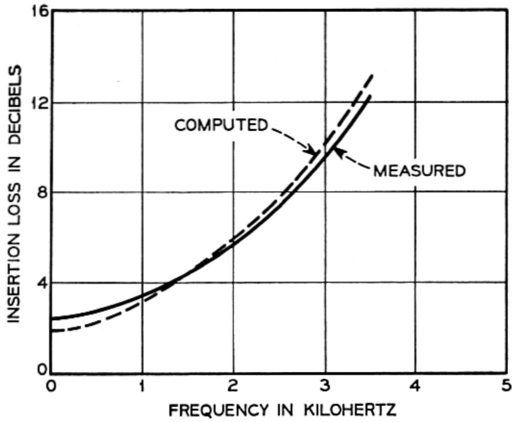

Fig. 10 — Insertion loss of 32-mile field-test NIB line between 225-ohm resistive terminations.

over them were favorably impressed by resemblance of the transmission to that over a short loop, and by freedom from noise, hum, crosstalk and distortion. Fig. 10 shows the insertion loss of one 32.4-mile line measured between 225 ohm resistive terminations. It also shows a computed plot of this loss, using a program that takes account of the individual dimensions of each section and NIB unit.

To help ensure stability in spite of the inherent restrictions on temperature compensation, the total copper resistance (6,000 ohms) was intentionally left undercompensated by about 100 ohms. As a result, the insertion loss had a low-frequency asymptote of roughly 2 dB. Strip chart records of a 1 kHz test tone showed the transmission varying over a typical day and night by about ±0.5 dB. Neither line lost stability at any time during the entire test, which extended over four fall and winter months and encountered large and rapid changes of weather.

Figure 11 shows the input impedance of one line, measured and computed, for a 225-ohm resistive far-end termination. The irregularities of these plots, resulting from nonuniformity of the sections, correspond to echo return losses no smaller than 12 dB, and exceeding 17 dB over most of the band.

Crosstalk loss between the two lines was roughly 88 dB at 1 kHz; there was little difference between near-end and far-end measurements.

In planning the field test, hum was of course recognized as a possible source of trouble. It was known that hum is generally introduced by magnetic induction from power lines, effectively generating equal voltages in series with each conductor. Longitudinal hum currents, impelled by these voltages, could trouble the NIB transmission in two ways: by using up a significant part of the operating range of the NIB units, and by coupling into the metallic circuit as a result of unbalance between the two sides of the line.

Experience and measurements afforded by the test were encouraging, but not extensive enough to be conclusive. In order to minimize hum currents, station grounds were avoided; the only path to ground was via capacitance distributed along the line. At the central office end, the longitudinal termination to ground was roughly matched to the longitudinal impedance of the line, to avoid possible accumulation of multiple reflections. With this arrangement line balance was found adequate to prevent more than a trivial hum level from ever being coupled into the telephones.

Hum voltage to ground (largely 60 Hz) recorded at the station end was found to vary from minute to minute as well as over a daily cycle. The extreme range of these measurements was from 1.8 to 6.5 volts rms, the largest values occurring around 5 to 6 pm. Without knowing the distribution of magnetic induction along the line, one could not determine hum current from such measurements. However,

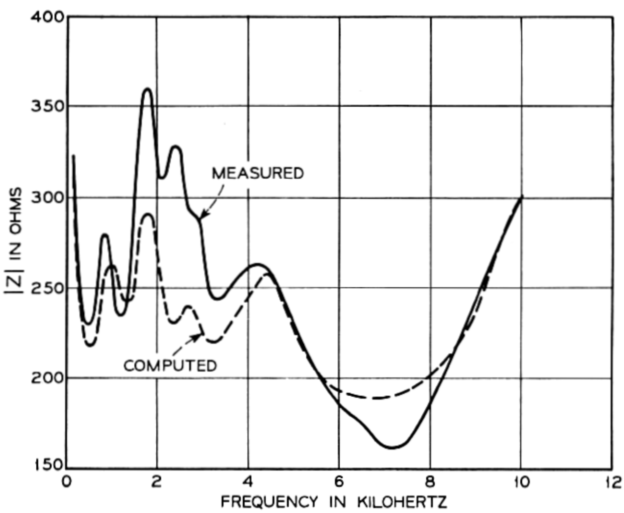

Fig. 11 — Input impedance of 32-mile NIB line with 225-ohm resistive far-end termination.

by varying the d-c loop current away from its usual 16 mA value until current peaks "bumped" an edge of the NIB dynamic range (putting audible 120 Hz pulses into the metallic circuit) one could readily measure the maximum hum current, reached at some boosting point along the line. Typical measurements of this sort gave values around 5 mA peak-to-peak in each conductor, or 25 per cent of the 20 mA dynamic range; under worst conditions at least half the range was undoubtedly filled. Although this amount of hum was found to have no noticeable effect on telephone speech, larger hum currents would probably be encountered at other locations.

Experience with lightning was also encouraging although far from comprehensive. The NIB units were left unprotected except by their own fairly low resistance at large forward currents, and by diodes to bypass reverse currents. No damage was done by thunderstorms, several of which did occur during the field run. Not until after these tests was it recognized that valid protection against large forward currents also could have been provided by merely giving each bypassing diode a zener potential of around 10 volts. Of course, this value is chosen to exceed the drop across the NIB at the "first bend" of its V–I plot. At large forward currents, the emitter and base circuit resistors of Fig. 1 combine to give a terminal resistance of about 48 ohms. With the terminal voltage zener-limited to 10 volts, the current through the NIB could not exceed 0.2 ampere, whereas simulated lightning tests have shown that an unprotected NIB is undamaged by surge currents as great as 5 amperes. Lightning is not expected to present a serious problem.

VI. BAND BROADENING

Shortly after conclusion of this field experiment continuing effort to improve the NIB circuit revealed that by adding to it a resistor and a capacitor, one could flatten and substantially broaden the resulting transmission band, indeed achieving virtually flat lossless transmission almost up to the frequency of quarter-wavelength NIB spacing. The band-broadened equivalent circuit, shown in Fig. 12, is simply that of the basic unit (Fig. 2) shunted by R_s and C_s in series.

The effect of the addition can be seen more readily if one first writes the impedance of the basic unit:

$$Z_A = R_A + jX_A = \frac{-R_n}{1 + (\omega T_n)^2} + R_p + j\omega \frac{T_n R_n}{1 + (\omega T_n)^2}. \tag{9}$$

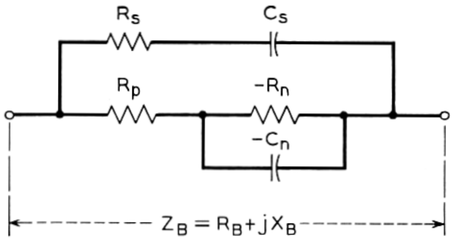

Fig. 12 — Equivalent circuit of NIB unit with band broadening.

When the shunt is applied, the real component R_B (negative) of the resulting terminal impedance Z_B is made larger than the real component R_A (also negative) of Z_A by what amounts to antiresonance between C_s and the positive (inductive) imaginary component of Z_A. Resistor R_s keeps the shunt path from acquiring so low an impedance at any frequency as to bring instability to the "open-circuit-stable" basic unit.

When the straightforward algebraic analysis used to derive expression (7) for the basic unit is repeated for the band-broadened circuit, it shows that the asymptotic low-frequency image impedance (for $G = 0$ and $\Sigma R = 0$) has been slightly modified. With the shunt elements added,

$$Z' = \lim_{\omega \to 0} Z_H = \sqrt{\frac{R_n T_n}{lC} + \frac{L}{C} - \frac{R^2 l^2}{12} - \frac{R^2 l T_s}{R_s C}}. \tag{10}$$

This expression reverts to (7) when $T_s \to 0$ with $R_s > 0$, or when $R_s \to \infty$ with finite T_s. Computer results confirm the accuracy of (10).

Computed transmission characteristics also support an initial estimate that the time constant $T_s = R_s C_s$ should be made roughly equal to T_n, and show that the revised circuit can be proportioned to sustain its compensation of copper resistance up to higher frequencies, while still letting its negative resistance fall off fast enough above the transmission band to preserve stability.

The effect of band broadening upon the NIB transmission is shown in Figs. 13 and 14 for the case of 22-gauge BSA cable with 12,000-foot NIB spacing, used earlier as an example. Here both time constants (T_s and T_n) are made 16 μs, and curves are shown for three values of R_s. When $R_s = 2{,}000\ \Omega$ the attenuation (Fig. 13) has its widest flat region without appreciable gain over any of the band. For $R_s = \infty$, the circuit reverts to the original or basic NIB. At an inter-

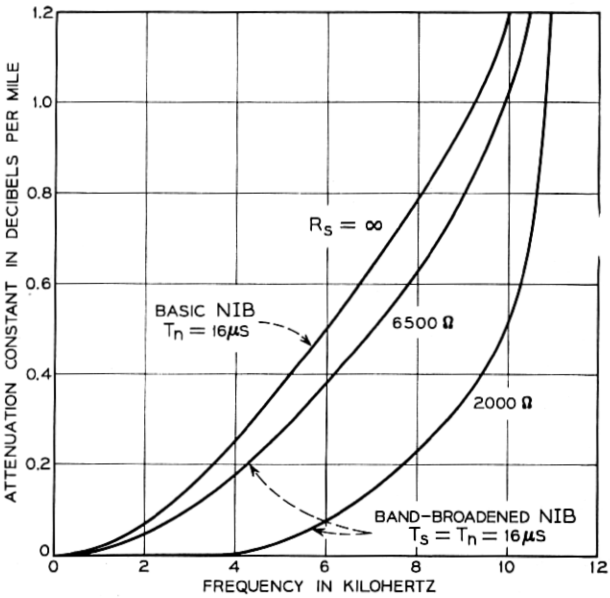

Fig. 13 — Effect of band broadening upon attenuation constant of NIB line; 22-gauge BSA cable, 12,000-foot spacing.

mediate value, $R_s = 6{,}500\ \Omega$, there is less band broadening, but the phase velocity (Fig. 14) becomes remarkably constant from zero frequency up to 6.7 kHz (at which $l = \lambda/4$). A similar change in slope of the phase velocity plot, shifting from positive sign for the basic NIB to negative for the band-broadened version, has consistently been observed over a wide variety of gauges and booster spacings.

VII. PULSE FORMING

The foregoing combination of linear variation of phase with an approximately parabolic variation of loss in dB, both as functions of frequency, clearly offers interesting possibilities in baseband pulse transmission. Under such a condition the line has the properties of a Gaussian filter. If rectangular pulses of a suitable width T and baud rate $f_o = 1/T$ are applied to it, these pulses are shaped in transmission into the raised cosine form. As received, they have the width T at half their peak amplitude and $2T$ along the baseline; they are almost free of tails. For ideal raised-cosine pulse forming, the line or Gaussian filter should have a loss of 1 neper or 8.68 dB at the baud rate f_o. Hence, for the case of R_s = 6,500 ohms in Figs. 13 and 14, a baud rate of 8 kHz (at which the loss is about 0.635 dB per mile) could be sent over a line 8.68/0.635 = 13.7 miles long. Of course if the line were shorter, or the baud rate slower, the pulses would still be symmetrical and well formed, but would show flatness at their peaks.

Figure 15 shows the output "eye-diagram" formed by a random sequence of 8-level rectangular pulses at a 16.67 kilobaud rate, sent over 10.2 miles of 22-gauge BSA cable, with 6,000-foot NIB spacing. Here the information rate was 3 times the baud rate, or 50 kilobits per second. The NIB parameters were R_p = 97.3 ohms, R_n = 293.9 ohms, $T_s = T_n = 6.1 \times 10^{-6}$ second and R_s = 2,000 ohms.

VIII. BIDIRECTIONAL TRANSMISSION

Because of low loss in a broad transmission band, and an image impedance that can be well matched over that band, new possibilities are opened of simultaneous bidirectional carrier transmission; for

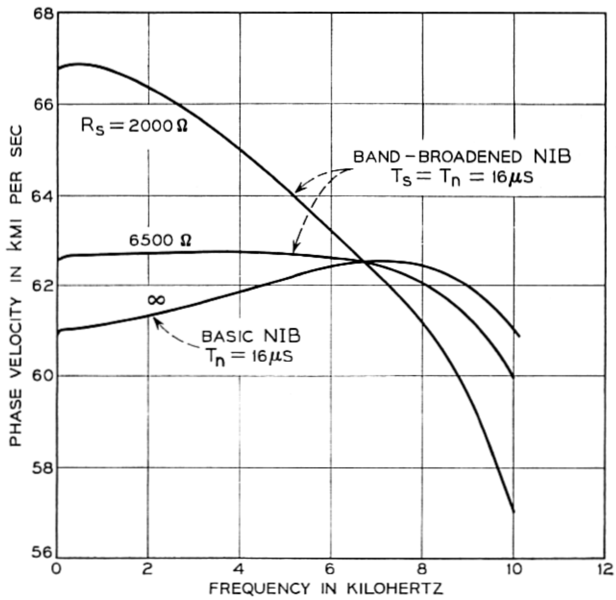

Fig. 14 — Effect of band broadening upon phase velocity of NIB line; 22-gauge BSA cable, 12,000-foot spacing.

example, by double-sideband amplitude modulation of the same carrier frequency at each terminal of the line. Similar possibilities exist for bidirectional baseband pulse transmission. Both of these schemes have been successfully carried out in the laboratory over the same 10.2-mile 22-gauge line with 6,000-foot spacing that was used in obtaining Fig. 15.

In either case, hybrid balance separates the incoming from the outgoing signal. As a result of the low transmission loss, the received signal, if it is a modulated carrier, is left sufficiently free of outgoing carrier (whatever its phase) to be detected without appreciable distortion. Similarly, if the received signal is a pulse train, it is left sufficiently free of interference from the outgoing pulses to be correctly decoded or regenerated.

Figure 16 shows two eye diagrams, received simultaneously at the two ends of the 10.2-mile line while two random 8-level pulse trains were being sent in the respective directions. Some interference may be seen in the interpulse intervals, resulting from imperfection of the hybrid balance presented to the higher frequency components of the rectangular input pulses. For this photograph, the pulse rate was raised slightly (to 16.81 kilobauds), thereby roughly centering the interference in the intervals between eyes of the diagram.

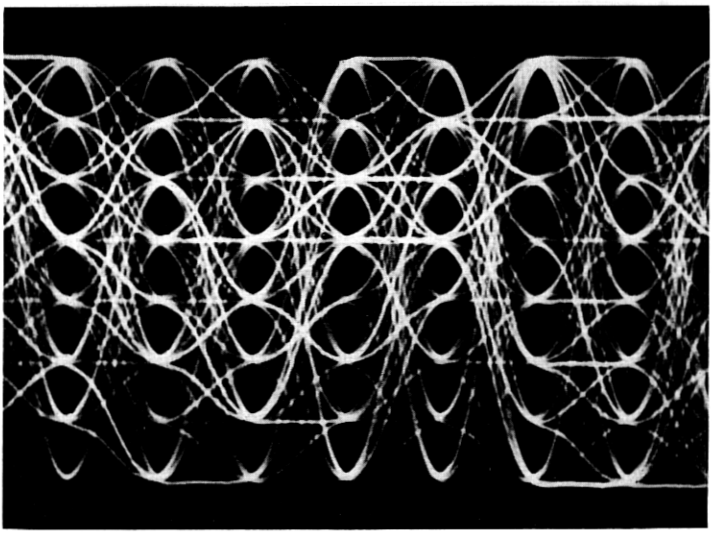

Fig. 15 — Eight-level pulses received over phase-linearized NIB line.

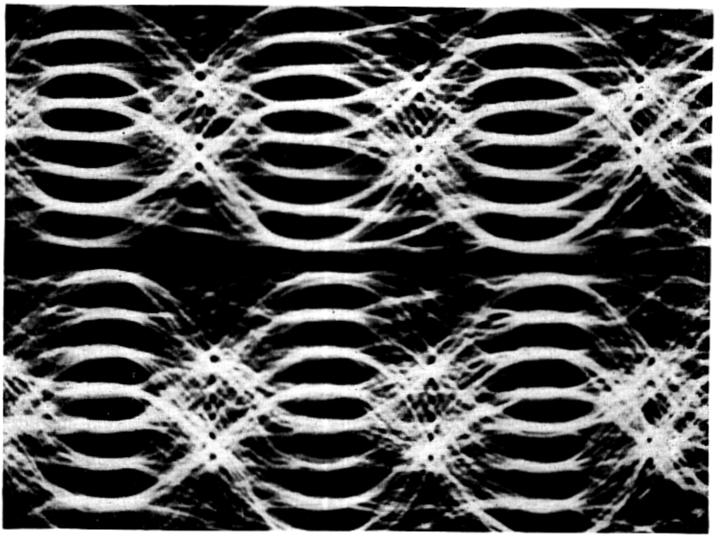

Fig. 16 — Bilateral pulse transmission over phase-linearized NIB line.

APPENDIX

Zero-frequency Asymptotes of Midspacing Image Impedance and Phase Velocity of NIB Lines

In this appendix derivations are given for expressions (7) and (8) of the text. The same method yields (10) when the NIB units include R_s and C_s as in Fig. 12.

Terms

Z_H = Midspacing image impedance of NIB line.
V_H = Phase velocity of NIB line.
Z_A = Total impedance of two NIB units, one on each side of balanced line, serving a single section.
l = Length of NIB section (miles).
Z_O = Characteristic impedance of nonloaded line.
$\gamma = \alpha + j\beta$ = Propagation constant of nonloaded line (per mile).
Z_{OC} = Open-circuit impedance of nonloaded half section (length $l/2$).
Z_{SC} = Short-circuit impedance of nonloaded half section (length $l/2$).
$T_n = R_n C_n$ = Time constant of basic NIB unit.
$lP = l(\alpha_H + j\beta_H)$ = Propagation constant of NIB line (per section).
$Z' = \lim_{\omega \to 0} Z_H$
$V' = \lim_{\omega \to 0} V_H$

Characteristic Impedance

From well-known theory,[4]

$$Z_H = Z_{OC}\sqrt{\frac{Z_A + 2Z_{SC}}{Z_A + 2Z_{OC}}} \tag{11}$$

$$Z_{OC} = \frac{Z_O}{\tanh \frac{\gamma l}{2}} \tag{12}$$

$$Z_{SC} = Z_O \tanh \frac{\gamma l}{2} \tag{13}$$

$$Z_O = \sqrt{\frac{R + j\omega L}{G + j\omega C}} = \frac{a}{b} \tag{14}$$

and

$$\gamma = \sqrt{(R + j\omega L)(G + j\omega C)} = ab \tag{15}$$

where

$$a^2 = R + j\omega L \quad \text{and} \quad b^2 = G + j\omega C. \tag{16}$$

Also

$$\tanh \frac{\gamma l}{2} = \left(\frac{\gamma l}{2}\right) - \frac{1}{3}\left(\frac{\gamma l}{2}\right)^3 + \frac{2}{15}\left(\frac{\gamma l}{2}\right)^5 - \cdots$$

$$= \frac{ablF}{2} \tag{17}$$

where

$$F = \left(1 - \frac{a^2b^2l^2}{12} + \frac{a^4b^4l^4}{120} - \cdots\right). \tag{18}$$

Then

$$Z_{OC} = \frac{2}{b^2lF} \tag{19}$$

$$Z_{SC} = \frac{a^2lF}{2} \tag{20}$$

and from (11),

$$Z_H^2 = \frac{4(Z_A + a^2lF)}{b^2lF(Z_Ab^2lF + 4)}. \tag{21}$$

From Fig. 2

$$Z_A = R_p - R_n \frac{(1 - j\omega T_n)}{1 + \omega^2 T_n^2}$$

$$= \frac{R_p + \omega^2 T_n^2 R_p - R_n + j\omega R_n T_n}{1 + \omega^2 T_n^2}$$

$$= S(R_p - R_n) + T_n S(\omega^2 R_p T_n + j\omega R_n) \tag{22}$$

where

$$S = \frac{1}{1 + \omega^2 T_n^2} = 1 - \omega^2 T_n^2 + \omega^4 T_n^4 - \cdots . \tag{23}$$

Putting (16) and (22) into (21) gives

$$Z_H^2 = \frac{4[S(R_p - R_n) + T_n S(\omega^2 R_p T_n + j\omega R_n) + (R + j\omega L) lF]}{(G + j\omega C) lF [S(R_p - R_n)(G + j\omega C) lF + T_n S(\omega^2 R_p T_n + j\omega R_n)(G + j\omega C) lF + 4]} . \tag{24}$$

Of present interest is the special case in which $G = 0$ and $R_p - R_n = -lR$. For this condition,

$$Z_H^2 = \frac{4[lR(F - S) + j\omega(lLF + R_n T_n S) + \omega^2 R_p T_n^2 S]}{j\omega C lF[4 - j\omega C l^2 RFS + j\omega C lF T_n S(\omega^2 R_p T_n + j\omega R_n)]} . \tag{25}$$

Consider now the term $F - S$ in the numerator of (25). From (18) and (23)

$$F - S = -\frac{a^2 b^2 l^2}{12} + \omega^2 T_n^2 + \frac{a^4 b^4 l^4}{120} - \omega^4 T_n^4 \cdots \tag{26}$$

and since $a^2 b^2 = j\omega RC - \omega^2 LC$

$$F - S = -\frac{j\omega l^2 RC}{12} + \omega^2 M\left(\frac{l^2 LC}{12} + T_n^2 - \frac{l^4 R^2 C^2}{120}\right) \tag{27}$$

where $M = 1 +$ terms of positive order in ω. Putting (27) into (25) gives

$$Z_H = \frac{4\left[\frac{-j\omega l^3 R^2 C}{12} + \omega^2 lRM\left(\frac{l^2 LC}{12} + T_n^2 - \frac{l^4 R^2 C^2}{120}\right) + j\omega\left(lLF + R_n T_n S\right) + \omega^2 R_p T_n^2 S\right]}{j\omega C lF[4 - j\omega C l^2 RF + j\omega C lF T_n S(\omega^2 R_p T_n + j\omega R_n)]}$$

$$= \frac{4\left[\frac{-l^2 R^2}{12} - j\omega RM\left(\frac{l^2 L}{12} + \frac{T_n^2}{C} - \frac{l^4 R^2 C}{120}\right) + \frac{LF}{C} + \frac{R_n T_n S}{lC} - \frac{j\omega R_p T_n^2 S}{lC}\right]}{F[4 - j\omega C l^2 RF + j\omega C lF T_n S(\omega^2 R_p T_n + j\omega R_n)]} . \tag{28}$$

Thus far, although F, S, and M are power series expansions, they are included in their entirety; nothing has been approximated, and (28) is therefore exact.

In passing to the zero-frequency limit we notice that when $G = 0$

$$\lim_{\omega \to 0} F = \lim_{\omega \to 0} S = \lim_{\omega \to 0} M = 1. \tag{29}$$

Accordingly, for the special case considered,

$$(Z')^2 = \lim_{\omega \to 0} Z_H^2 = \frac{4\left[-\dfrac{l^2R^2}{12} - 0 + \dfrac{L(1)}{C} + \dfrac{R_nT_n(1)}{lC} - 0\right]}{(1)[4 - 0 + 0]}$$

$$= \frac{R_nT_n}{lC} + \frac{L}{C} - \frac{l^2R^2}{12}. \tag{30}$$

Phase Velocity

Again from well-known theory,[4]

$$\tanh \frac{lP}{2} = \frac{Z_H}{Z_{OC}}. \tag{31}$$

From (30) the zero-frequency limit of Z_H is finite, real and presumed positive, while from (19) that of Z_{OC} (for $G = 0$) is infinite, imaginary and negative. Hence as $\omega \to 0$,

$$\frac{Z_H}{Z_{OC}} = \tan \frac{lP}{2} \to \frac{lP}{2} \to \frac{j\beta_H l}{2} \to 0. \tag{32}$$

Accordingly,

$$\lim_{\omega \to 0} \beta_H = \lim_{\omega \to 0} \frac{2Z_H}{jlZ_{OC}}, \tag{33}$$

and since $V_H = \omega/\beta_H$,

$$\lim_{\omega \to 0} V_H = \lim_{\omega \to 0} \frac{j\omega l Z_{OC}}{2Z_H}. \tag{34}$$

But from (12), with $G = 0$

$$Z_{OC} = \frac{2}{j\omega C l F},$$

and therefore

$$\lim_{\omega \to 0} V_H = \frac{1}{C} \lim_{\omega \to 0} \frac{1}{Z_H}. \tag{35}$$

REFERENCES

1. Heaviside, Oliver, "Electromagnetic Induction and Its Propagation," Electrician, *40* (June 3, 1887), pp. 79–81.

2. Bullington, R. K., "Negative Resistance Loading," U. S. Patent 2,360,932, April 25, 1942.
3. Miller, S. L. and Ebers, J. J., "Alloyed Junction Avalanche Transistors," B.S.T.J., *34,* No. 5 (September 1955), pp. 883–902.
4. Merrill, J. L., Rose, A. F., and Smethurst, J. O., "Negative Impedance Telephone Repeaters," B.S.T.J., *33,* No. 5 (September 1954), pp. 1055–1092.
5. Gammie, J. and Merrill, J. L., Jr., "Stability of Negative Impedance Elements in Short Transmission Lines," B.S.T.J., *34* No. 2 (March 1955), pp. 333–360.
6. Meacham, L. A., Power, J. R., and West, F., "Tone Ringing and Pushbutton Calling," B.S.T.J., *37,* No. 2 (March 1958), pp. 339–360.